1
Introduction

1.1
Some Historical Remarks

In spite of the fact that some types of particle accelerators had been invented before the second war of the last century, the real boom of building these facilities for the production of high-energy beams started after the war. The original motivation was the extension of the basic nuclear physics research into the field of particle physics. While some applications of medium-energy beams for medical purposes and isotope production had been anticipated, the main motivation to build these machines was fundamental research.

Nuclear reactors – a typical child of defense work during the war – had been built in order to produce fissile materials and with the prospect to become useful as power stations after the war. Their usefulness as neutron sources for basic research for the physics of condensed matter was, however, immediately recognized. As soon as neutron beams from so-called piles became available, the first diffraction experiments for the investigation of crystal structures, as an alternative to Bragg scattering at X-ray tubes, were realized [1, 2]. Subsequently, dedicated beam tube reactors became the standard neutron sources for this type of research [3].

That was the situation in the 1960s

- nuclear beam tube reactors for neutrons, and
- ever improving X-ray tubes for hard photons, and
- nobody had yet ordered muons for solid-state physics.

This situation was then confronted by an inexhaustible claim of the experimentalists for higher flux, bigger luminosities, and higher flexibilities driven by ever higher ambitions of the experimental goals and their setup.

In the meantime, nuclear research reactors were, however, approaching their technical limits. For increase of the experimentally useful neutron, a new approach was needed, and this came from the accelerator fission process, which was an alternative method to produce free neutrons – namely the spallation reaction [4]. In this reaction, nuclei in a heavy (normally nonfissile) metal target, bombarded by medium–high energy protons (as we would say today), will be highly excited to the

X-Rays, Neutrons and Muons: Photons and Particles for Material Characterization,
First Edition. Walter E. Fischer.

extent that they evaporate many of their neutrons. With a proton accelerator within an energy range of say 600 MeV–2 GeV, but with an intensity as high as possible, neutron sources of this kind became feasible. With a fast cycling proton synchrotron such a system gives a pulsed spallation neutron source, the most prominent type in use today. Using as accelerator a cyclotron which produces a continuous proton beam a steady neutron source is also feasible. These accelerators of medium energy and high intensity with beam power up to a megawatt served the nuclear and particle physics community as pion factories.

The π-meson, being responsible for the longer range part of nuclear forces, is unstable and decays into a muon and a neutrino. The muon (see Chapter 2) had been discovered before as a component in cosmic rays and became a prominent object of research for particle physics. Their experiments aiming mostly for extremely high precisions were often plagued by the muon interaction with the rest-gas or the detector materials. These effects – felt as a nuisance originally – are the origin of the muons as a probe of condensed matter.

Strangely enough the signification of the synchrotron radiation has a similar origin. Of course optical methods played always a prominent role in the experimental investigations of condensed matter. As the name says they were somewhat restricted to the spectral range between infrared and ultraviolet. Particular progress was of course achieved by the invention of the lasers as the primary light source. X-ray tubes served as light sources for laboratory experiments in the harder spectral region.

Synchrotron radiation which is unavoidable in a circular electron accelerator was considered to be plague since much of the energy pumped into the beam is immediately radiated off into the vacuum chamber. Hence the later high energy machines for particle physics were built as linear accelerators. Attempts to extract a synchrotron light beam from a circular machine tangential to the electron beam in a bending magnet already showed the potential of this principle to produce useful light beams over a broad spectral range up to soft X-rays depending on the energy of the electron beam and the bending strength of the magnet. This then led to a rapid development of several generations of dedicated synchrotrons and storage rings for the production of these light beams for the physics of condensed matter. The present generation of these facilities includes now also amplification insertion devices like wigglers and undulators.

1.2 The Experimental Methods

For an instructive experiment the following two conditions ought to be fulfilled:

- The probe should not alter in an unknown or uncontrollable fashion due to the effect under study.
- We need a clear idea about how to interpret the results of measurement.

Both conditions are connected with the weakness of the interaction between the probe and constituents of the sample. This allows us in a scattering experiment to

restrict to kinematical scattering that is, to neglect multiple scattering. Response and perturbation are then linearly connected. Of course, this is not only a condition for the basic interaction but is also connected with some properties of the target. We shall come back to this point below.

While the probe does not affect the "integrity" of the sample, it is allowed to excite all the internal degrees of freedom of the sample within one scattering process. Due to the linear response, mathematical interpretation becomes straightforward. Thermal neutrons and X-rays are typical examples for this kind of probes, since they do not carry an electric charge which could distort the lattice. Furthermore, since we are usually interested in an atomic resolution down to say 1 Å, they carry the appropriate wavelength (see Chapter 2). Hence prominent types of experiments are:

- **Diffraction of X-rays or neutrons**: There exists nearly a one-to-one relationship between the angular distribution of the scattering intensity and the electron-resp. nuclear-density distribution in the unit cell (see Section 4.3.4).
- **Inelastic scattering of neutrons or X-rays**: They give information about well-defined excitations in solids (see Section 4.3.5).

As an example, we show in Figure 1.1 the setup of an inelastic neutron-scattering experiment. A corresponding arrangement may also be imagined for X-rays as a probe. The experiment starts with a monochromatic beam and analyses the final neutron energy after the scattering process. If appropriate, for instance, at a pulsed neutron source, either of two crystal selectors may (for neutrons only) be replaced by a

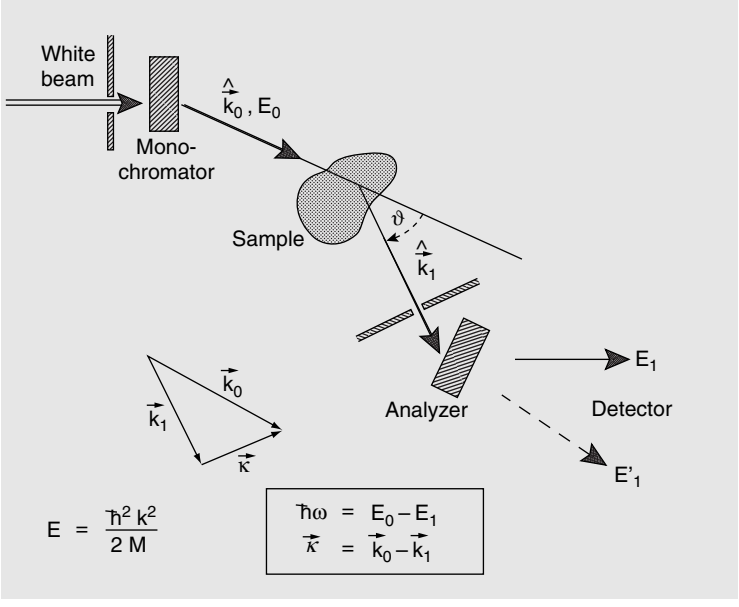

Figure 1.1 Setup of an inelastic neutron-scattering experiment.

time-of-flight configuration. The energy- and momentum-transfer variables

$$\hbar\omega = E_0 - E_1 \tag{1.1}$$

$$\vec{\kappa} = \vec{k}_0 - \vec{k}_1 \tag{1.2}$$

define the kinematics of the scattering event. $\left(E_0, \vec{k}_0\right)$ and $\left(E_1, \vec{k}_1\right)$ are the energy and the wave vector of the incident and escaping probe, respectively. The kinematics of this process shall be discussed in more detail in Section 4.3.5. For the time being, let us just give here as in Figure 1.2 the kinematical domain of the energy and momentum transfer for neutron scattering. Elastic-scattering event sits on the axis with $\hbar\omega = 0$, while the upper and lower parts of the domain are populated by inelastic events. If the sample is at zero temperature, only energy transfer from the probe to the sample is possible, the maximum being given by the kinetic energy of the probe (Stokes). In the lower part the transfer is reversed, which is of course only possible if the excited states of the sample are populated that is, if the sample is at higher temperature (anti-Stokes). Note the analogy to optical Raman scattering.

In Table 1.1 we give notions and ingredients of typical scattering experiments. The differential cross-section populating the kinematical domain shown in Figure 1.2 turns out to be proportional to a scattering function $S(\omega, \vec{\kappa})$ essentially due to L. van Hove [5] which completely fulfils our two conditions, that the probe should not alter in an unknown fashion and that we should have a clear idea about the interpretation of the experiment. Chapter 4 will be nearly entirely dedicated to this central notion.

Concerning the characterization of the sample a few remarks are still in order.

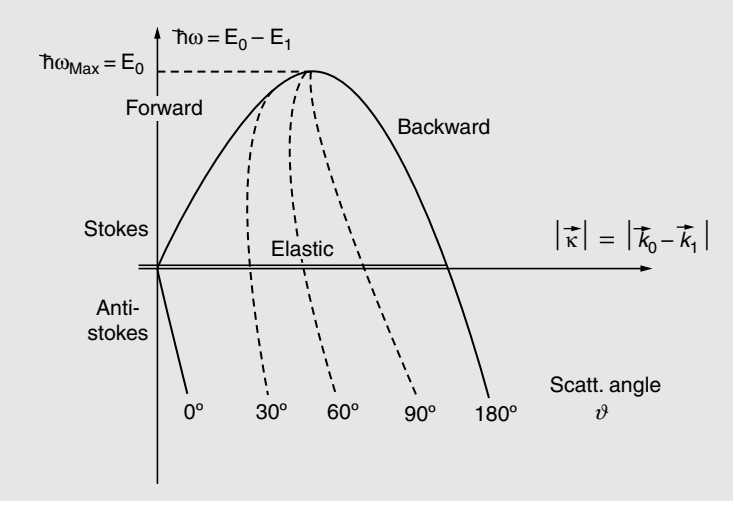

Figure 1.2 Kinematical domain of the energy and momentum transfer for neutron scattering. A detailed discussion of the scattering process is given in Section 4.3.5.

Table 1.1 Concept of a scattering experiment and the parameters which influence the measurement.

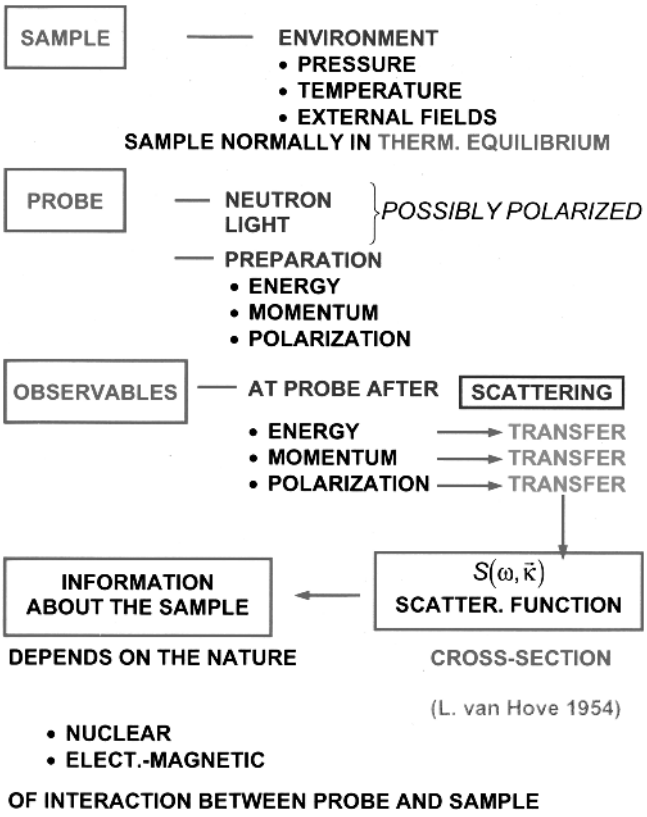

Clearly, the sample should be large enough so that it can be represented as a bulk that is, as a three-dimensional object with its corresponding properties. Surface effects which normally differ from the bulk should be negligible. On the other hand, the sample ought to be small enough – and this now depends on the strength of the interaction with the probe – that we can neglect multiple scattering.

We assume that the target is either in a liquid or a solid state (condensed matter), although a gaseous phase is in principle also possible. The temperature range is considered to be between a few thousand Kelvin down to (as near as possible) absolute zero. This implies that the scattering centers, which we call here basic constituents (nuclei, atoms), are usually not thermally excited – hence are initially in their ground state before the scattering process starts.

This may well change during the scattering process for atomic degrees of freedom in the case of X-rays, probing the sample. Due to their low incident energy this is not so for neutrons and muons.

The initial state of the sample is usually a stationary state, or more often even a thermodynamic equilibrium with a well-defined temperature. Other extensive parameters, as indicated in Table 1.1 may control the state statically, e.g., pressure and external magnetic or electrical fields. Note that all these conditions require a particular material environment of the samples such as

- cryostats
- ovens
- pressure cells, etc.

Their material may influence the experimental data and become an important concern while interpreting the results.

Let us finally say a few words about the muon as a probe.

The principle of a μSR experiment (muon spin rotation/relaxation/resonance) is described in Appendix E. Clearly, the implantation of a muon with its electrical charge into the sample acts like a defect in the lattice that is, it polarizes its environment. While the muon charge may cause some complications, it opens up, on the other hand, a great opportunity to the experimental control of the beam. By means of electrostatic lenses we can achieve a geometrical control of the beam spot on the sample. Furthermore, by controlling the beam energy we may determine the penetration depth of the muon into the sample. This opens up unique possibilities to investigate, for example, the distribution of magnetization through surfaces or even multilayered systems.

1.3 The Solid as a Many Body

In order to attune ourselves into the subject, let us give here initially a general description of the sample. Thereby we take into account that its constituents and therefore the sample as a whole consist of positively charged nuclei carrying most of the mass and negatively charged electrons. The forces between these particles are given by a potential $V(\vec{x}, \vec{X})$, where $\vec{x}$ stands for all the electronic coordinates and $\vec{X}$ correspondingly for the nuclei. We assume V to be described by a sum (see Sections 4.2–4.4) of electrostatic forces, namely between

- electrons–electrons
- ions–ions
- electrons–ions.

The sample ought to be described by the Schrödinger equation

$$\left[T^{(i)} + T^{(e)} + V(\vec{x}, \vec{X})\right]\Phi(\vec{x}, \vec{X}) = E\Phi(\vec{x}, \vec{X}) \tag{1.3}$$

where

$$T^{(i)} = -\sum_i \frac{\hbar^2}{2M}\vec{\nabla}^2_{\vec{X}_i} \quad \text{and} \quad T^{(e)} = -\sum_j \frac{\hbar^2}{2m}\vec{\nabla}^2_{\vec{x}_j} \tag{1.4}$$

are the operators for the kinetic energy of the ions and the electrons, respectively. Note that for simplicity we just deal with one type of nucleus. We now seek a solution of the form

$$\Phi(\vec{x},\vec{X}) = \sum_n \phi_n(\vec{X})\varphi_n(\vec{x},\vec{X}) \tag{1.5}$$

The complete system φ_n serving as a basis of Φ describes the electrons, which their amplitudes ϕ_n form the wavefunction of the ions. We assume both systems to be orthogonal. If we now insert (1.5) into (1.3) and project onto $\langle\varphi_m|$, we obtain the two equations

$$\left[T^{(e)} + V(\vec{x},\vec{X})\right]\varphi_n(\vec{x},\vec{X}) = E_n^{(0)}(\vec{X})\varphi_n(\vec{x},\vec{X}) \tag{1.6}$$

$$\sum_n \langle\varphi_m|T^{(i)}\phi_n(\vec{X})|\varphi_n\rangle + E_m^{(0)}(\vec{X})\phi_m(\vec{X}) = E\phi_m(\vec{X}) \tag{1.7}$$

which are equivalent to (1.3). Equation (1.6) describes the electronic motion and contains the ionic coordinates only as parameters, whereas the ionic equation(1.7) by its first term still couples electronic and ionic degrees of freedom. It consists of three parts:

$$\vec{\nabla}_{\vec{X}}^2\phi_m(\vec{X}) \tag{1.8}$$

$$\left(\vec{\nabla}_{\vec{X}}\phi_n(\vec{X})\right)\left\langle\varphi_m\middle|\vec{\nabla}_{\vec{X}}\middle|\varphi_n\right\rangle + \left\langle\varphi_m\middle|\vec{\nabla}_{\vec{X}}\middle|\varphi_n\right\rangle\left(\vec{\nabla}_{\vec{X}}\phi_n(\vec{X})\right) \tag{1.9}$$

$$\phi_n(\vec{X})\langle\varphi_m|\vec{\nabla}_{\vec{X}}^2|\varphi_n\rangle \tag{1.10}$$

Separating them we can write (1.7) in the form

$$T^{(i)}\phi_m(\vec{X}) + \sum_n A_{mn}(\vec{X})\phi_n(\vec{X}) = \left(E - E_m^{(0)}(\vec{X})\right)\phi_m(\vec{X}) \tag{1.11}$$

with

$$A_{mn} = \langle\varphi_m|T^{(i)}|\varphi_n\rangle - \frac{\hbar^2}{M}\sum_i \langle\varphi_m|\vec{\nabla}_{\vec{X}_i}|\varphi_n\rangle\vec{\nabla}_{\vec{X}_i} \tag{1.12}$$

We recognize that the elements A_{mn} express the coupling of the motion of the nuclei with the electronic states. If we neglect all these terms, then Eqs. (1.6) and (1.11) are decoupled. In this case, the solution for the total wavefunction is of the form

$$\Phi(\vec{x},\vec{X}) = \phi(\vec{X})\varphi(\vec{x},\vec{X}) \tag{1.13}$$

This is the so-called Born–Oppenheimer (BO) approximation, which is often used in Quantum Chemistry and Molecular Spectroscopy. In this approximation, any motion of the ions is instantaneously followed by the electrons in exactly the same configuration. In view of the large mass difference between the ions and electrons this is a plausible approach. Note, however, that in this model there is no interaction between electrons and lattice vibrations.

The next step in sophistication is to take into consideration the diagonal elements of the matrix A, but it still neglects the nondiagonal elements. This is known as *adiabatic* approximation. Furthermore, in absence of a static magnetic field, the wavefunctions φ_n can be chosen to be real. The diagonal part of the second term of (1.12) is

$$\langle\varphi_n|\vec{\nabla}_{\vec{X}}|\varphi_n\rangle = \frac{1}{2}\vec{\nabla}_{\vec{X}}\langle\varphi_n|\varphi_n\rangle = 0 \tag{1.14}$$

since $\vec{\nabla}_{\vec{X}}$ cannot change the norm of the basis vectors. For the first term, by using

$$0 = \vec{\nabla}^2_{\vec{X}}\langle\varphi_n|\varphi_n\rangle = 2\int\varphi_n(\vec{\nabla}^2_{\vec{x}}\varphi_n)d^3x + 2\int(\vec{\nabla}_{\vec{x}}\varphi_n)^2 d^3x \tag{1.15}$$

we obtain

$$A_{nn} = \sum_i \frac{\hbar^2}{2M}\int(\vec{\nabla}_{\vec{X}_i}\varphi_n)^2 d^3x \tag{1.16}$$

For tightly bound electrons A_{nn} is $^m/_M$ times the kinetic energy of the electrons averaged over the motion. It just modifies the potential $E_n^{(0)}(\vec{X})$ by a small $O(^m/_M)$ correction. Including this term into the potential, we obtain

$$U(\vec{X}) = E_n^{(0)}(\vec{X}) + \sum_i \frac{\hbar^2}{2M}\int\left(\vec{\nabla}_{\vec{X}_i}\varphi_n\right)^2 d^3x \tag{1.17}$$

We can write for the ionic equation

$$\left[T^{(i)} + U(\vec{X})\right]\phi_n(\vec{X}) = E\phi_n(\vec{X}) \tag{1.18}$$

where $U(\vec{X})$ acts as an effective potential for the ionic motion with the first-order electronic correction (as we shall see immediately). In this adiabatic approximation the electronic energy $E_n^{(0)}$ is slightly shifted, but the nuclear motion does not mix up different electronic states. This electronic wavefunction follows the nuclear motion adiabatically and in a reversible way and stays always on the same potential surface.

In these approximations, the sample is characterized by two spectroscopic domains which are only very weakly coupled:

- the electronic degrees of freedom at rather high energies $O\,(\mathrm{eV})$ at a swift timescale and
- the comparatively sluggish motions of the ions at lower energies $O\,(10\,\mathrm{meV})$.

This is of course a consequence of the smallness of the mass ratio $(^m/_M)$. These two domains are connected by the nondiagonal matrix elements $A_{mn}(n \neq m)$ which we have neglected

$$A_{mn} = \langle\varphi_m|T^{(i)}|\varphi_n\rangle - \frac{\hbar^2}{M}\sum_i\langle\varphi_m|\vec{\nabla}_{\vec{X}_i}|\varphi_n\rangle\vec{\nabla}_{\vec{X}_i} \tag{1.19}$$

where A_{mn} describes the residual interaction between electrons and ions. This contribution to the lattice energy should show up in a second-order perturbation theory. With A_{mn} (1.19) as a perturbation of the nuclear kinetic energy and assuming

the BO approximation of zero order, the adiabatic correction consists only of the diagonal term of $\vec{\nabla}_{\vec{X}}$, that is A_{nn}. In higher order, we have

$$\phi_n = \phi_n^{(0)} + \lambda\phi_n^{(1)} + \lambda^2\phi_n^{(2)} + \cdots \tag{1.20}$$

for the nuclear wavefunction and for the energy

$$E_n = E_n^{(0)} + \lambda E_n^{(1)} + \lambda^2 E^{(2)} + \cdots \tag{1.21}$$

A convenient choice for λ is $\lambda = \left(\frac{m}{M}\right)^{\frac{1}{4}}$ [6]. From (1.11) we then obtain

$$E_n = E_n^{(0)} + A_{nn} + \sum_{k\neq n} \frac{A_{nk}A_{kn}}{E_n^{(0)} - E_k^{(0)}} + O\left(\lambda^3\right) + \cdots \tag{1.22}$$

The smallness of λ guarantees that the nondiagonal terms in (1.19) can be neglected as well, provided $\left(E_n^{(0)} - E_k^{(0)}\right)$ is large. Since the electronic excitations are of higher frequency than the lattice vibrations, this condition is normally fulfilled.

However, for degenerate or nearly degenerate electronic levels, this second-order term may be the cause of the breakdown of the adiabatic approximation. Electronic and ionic degrees of freedom couple with each other – a phenomenon which is described by electron–phonon interaction.

1.4
Survey over the Spectral Region of a Solid

As mentioned above, the differential cross-section of a scattering experiment with a weakly interacting probe is proportional to a scattering function $S(\omega, \vec{\kappa})$, where the momentum and energy transfer are given by (1.2) and (1.1), respectively. It will be shown in Section 4.4 that $S(\omega, \vec{\kappa})$ is the temporal and spatial Fourier transform of a correlation function $C(\vec{x}, t)$ in spacetime, where $\vec{x}$ stands for the positions of the scattering constituents as introduced in Section 1.3. Of course one cannot deal with all these coordinates – their number being of the order of $10^{23}\,\mathrm{cm}^{-3}$. Hence, C has to be understood as an average over a statistical ensemble. The correspondence defined by the Fourier transform between these two sets of variables can be expressed in the following way:

$$\boxed{\begin{array}{c} S(\omega, \vec{\kappa}) \\ \text{Excitations of internal degrees of freedom} \end{array}} \quad \leftrightarrow \quad \boxed{\begin{array}{c} C(\vec{x}, t) \\ \text{Fluctuations in space and time} \end{array}}$$

The nature of the fluctuations depends on the sensitivities of the probe. These are for

Neutrons:	Mass and magnetic density
X-rays:	Charge density
Muons:	Magnetization density
(As local probe $S(\omega, \vec{0})$)	

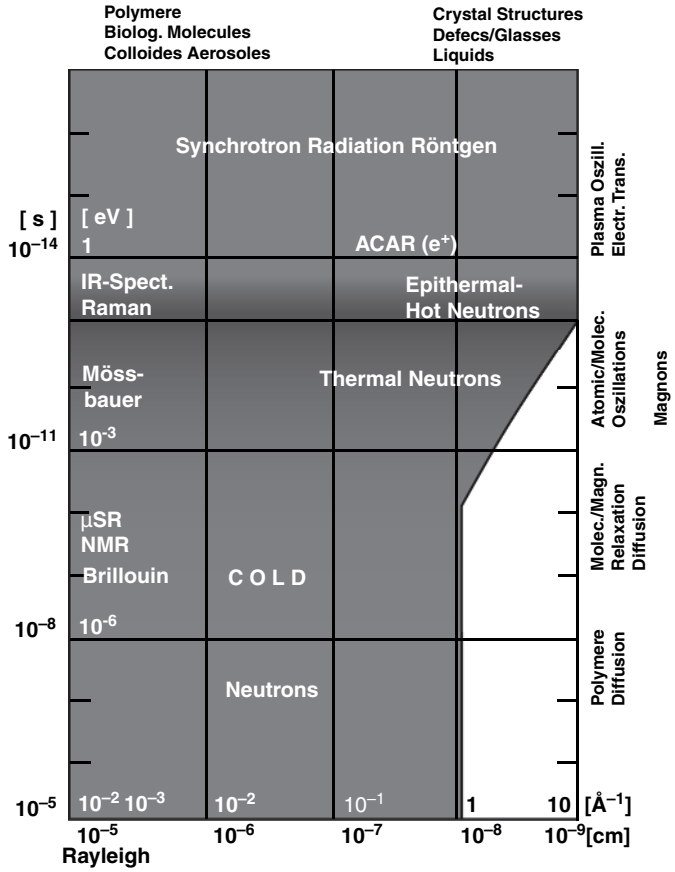

Figure 1.3 Access to space-time correlations by various experimental methods.

In Figure 1.3 we present a rough survey of the various phenomena which may be investigated by one or the other probe in the corresponding region of $(\omega, \vec{\kappa})$. The horizontal axis covers the momentum transfer $|\vec{\kappa}|$ from 10^{-3} to 10 Å^{-1} which corresponds to the resolutions of 10^{-5}–10^{-9} cm. This contains normally the first Brillouin zone with its center to the left. The vertical axis covers the energy transfer of inelastic scattering that is, for spectroscopic investigations from 10^{-9} eV up to some keV.

Coherent elastic scattering (strictly speaking with $\Delta\omega = 0$) results in Bragg reflections which are indicative for the structure of a periodic lattice. In praxis, these investigations are done on diffractometers without energy analysis at all. As indicated on top of this figure, the structures which may be resolved are on the atomic scale for large momentum transfer up to the mesoscopic domain for low momentum transfer (small angle scattering) which determines form factors, for example, with X-rays for mapping the electronic density.

The spectroscopic phenomena accessible with our probes are on the right vertical axis. The energy scale covered corresponds to correlation – and relaxation – times

between 10^{-9} and 10^{-16} s. The experimental methods indicated on the left are so-called local methods, either because they act really locally like μSR and normally also like NMR, or as optical methods as the energy of the probe being limited and hence its range in the reciprocal lattice constraints to $S(\omega, \vec{0})$.

A striking feature of Figure 1.3 is its separation into a lower part, which is dominantly influenced by the inertia of the ions. The upper part, corresponding to higher energies and faster relaxations, is described by electronic degrees of freedom. Such a separation is, of course, suggested by the validity of the BO or adiabatic approximation. This also reflects a partial complementarity of neutrons and X-rays as probes for the investigation of condensed matter. Of course, the intermediate region is of high interest for either probe, since that is where electronic and ionic degrees of freedom may mix up, which must have a strong influence on the temperature-dependent transport properties in solids.

The most upper region in Figure 1.3 involves core electrons and is strongly influenced by the atomic properties of the constituents. This is also the energy region of resonant X-ray scattering, which serves as a powerful tool to observe small signals by means of amplified interference terms. Clearly, that domain is hardly impressed by the kinetic energy of a thermal neutron.

References

1 Wollan, E.O. and Shull, C.G. (1948) The diffraction of neutrons by crystalline powders. *Phys. Rev.*, **73**, 830.

2 Wollan, E.O., Shull, C.G., and Marney, M.C. (1948) Laue photography of neutron diffraction. *Phys. Rev.*, **73**, 527.

3 Carpenter, J.M. and Yelon, W.B. (1986) Neutron Sources, in *Methods of Experimental Physics*, Volume 23A: Neutron *Scattering* (eds K. Sköld and D.L. Price), Academic Press, Orlando.

4 Carpenter, J.M. (1977) Pulsed spallation neutron sources for slow neutron scattering. *Nucl. Instrum. Methods*, **145**, 91–113.

5 van Hove, L. (1954) Correlations in space and time and Born approximation scattering in systems of interacting particles. *Phys. Rev.*, **95**, 249.

6 Born, M. and Oppenheimer, R. (1927) Zur Quantentheorie der Molekeln. *Ann. Phys.*, **389**, 457–484.